Exploring new Fundamental Physics by Precision Spectroscopy of Cold Molecules

«WHAT NEXT» MEETING

Pasquale Maddaloni

Firenze - May 4, 2015

Starting from *Puzzles*

Electron's electric dipole moment

Why does the Universe have so little anti-matter?

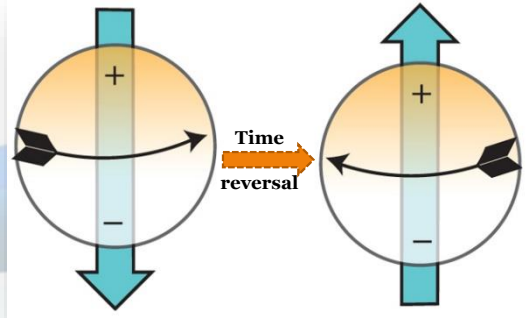

Variation of fundamental constants

Can Gravity be unified with other interactions?

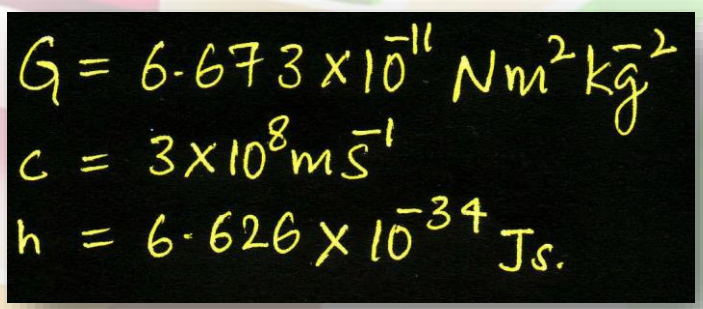

Parity violation

Why are life macromolecules homochiral?

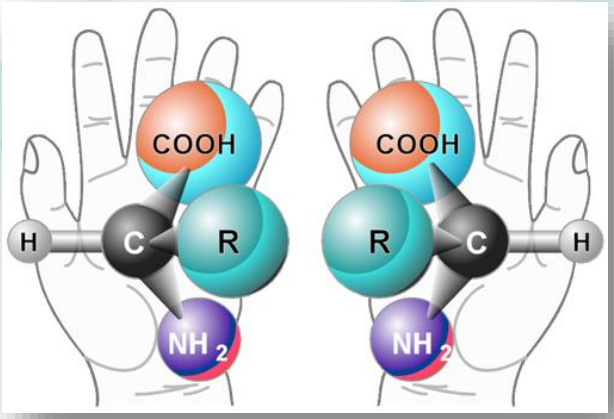

Axion dark matter

What is dark matter?

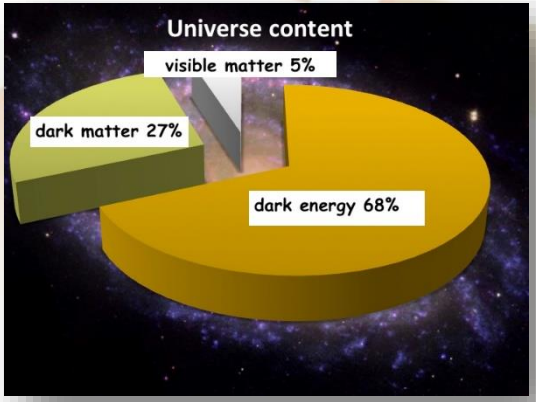

Electron's EDM measurement

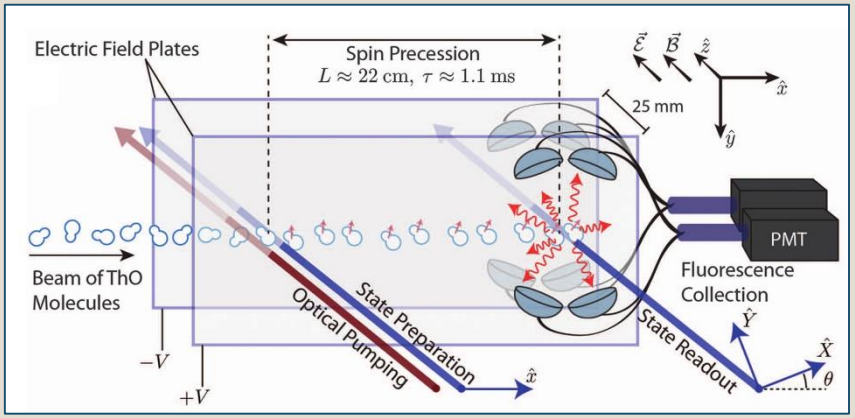

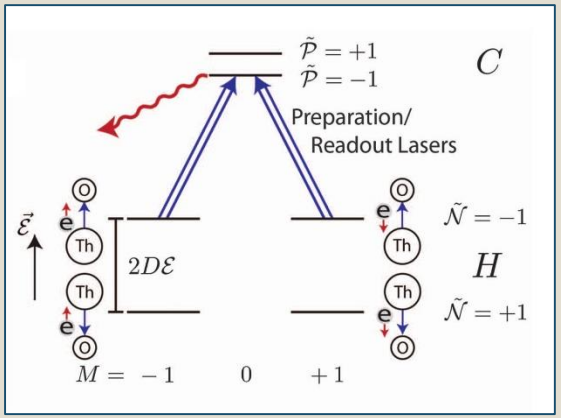

📖 J. Baron et al., Science **343**, 269 (2014)

ThO $\Longrightarrow |d_e| < 8.7 \times 10^{-29}\ e\,\text{cm}$ (90% confidence)

Extensions to the Standard Model, such as weak-scale supersymmetry, posit the existence of new particles and interactions that are asymmetric under time reversal (T) and nearly always predict a small yet potentially measurable electron electric dipole moment in the range of 10^{-27} to 10^{-30} e·cm. The size of the EDM is also intimately related to the question of why the Universe has so little antimatter. If the reason is that some undiscovered particle interaction breaks the symmetry between matter and antimatter, this should result in a measurable EDM in most models of particle physics.

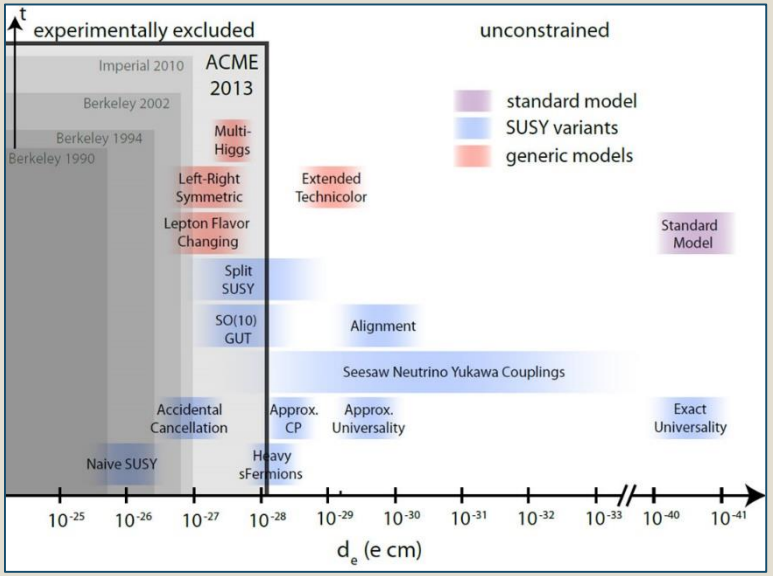

Axion dark matter detection

Axion dark matter detection by laser spectroscopy of ultracold molecular oxygen

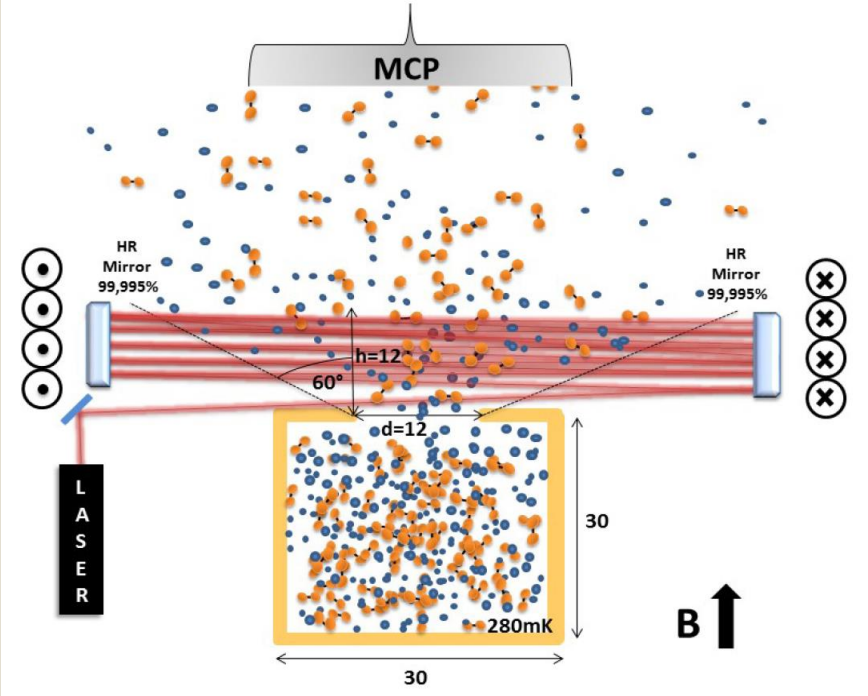

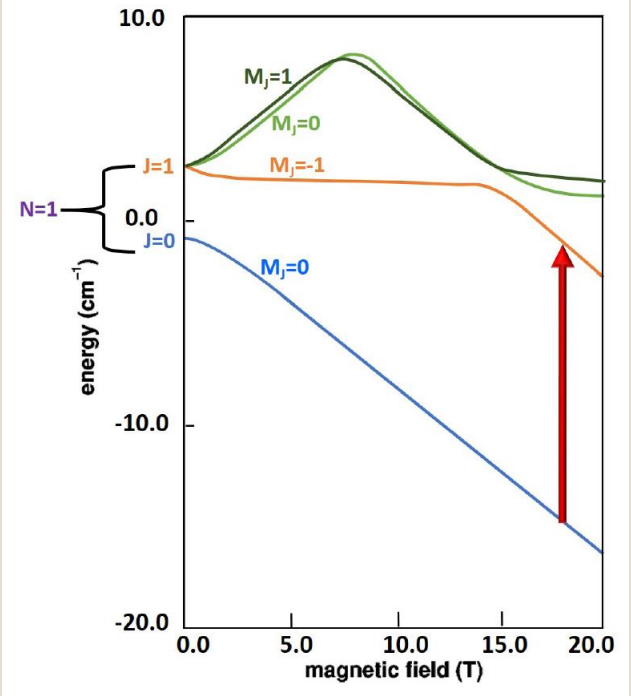

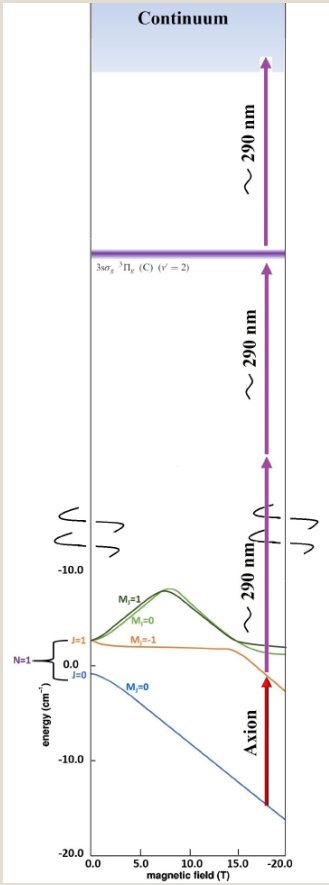

📖 L. Santamaria et al., *in preparation*

Parity violation in chiral molecules

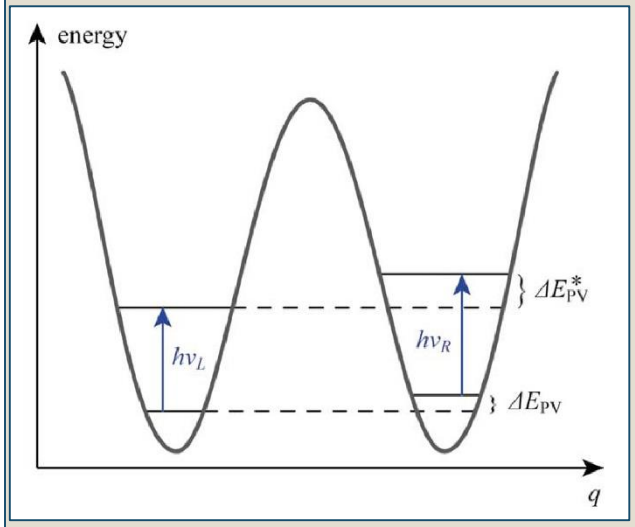

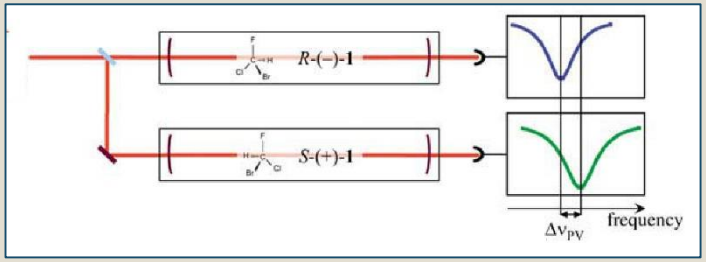

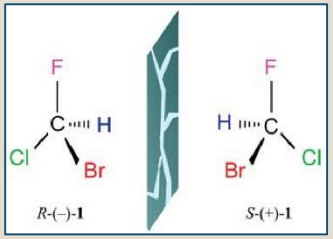

CHFClBr @ 9.3 μm ⟹ $5\cdot10^{-14}$ 🕮 B. Darquie et al., Chirality **22**, 870 (2010)

The potential energy surface of a chiral molecule shows two minima (as a function of the inversion coordinate q), that are the left "L" and right "R" enantiomers. In the presence of a weak force between nuclei and electrons, a small parity violation energy difference is expected between the ground states (as well as excited states) of the enantiomers: R- and L-handed molecules cease to be exact mirror images of each other. For CHFClBr, $\Delta\nu_{PV}=\nu_L-\nu_R=(\Delta E^*_{PV}-\Delta E_{PV})/h$ is such that $\Delta\nu_{PV}/\nu\sim10^{-16}$.

ALTERNATIVE APPROACHES

- Study time-dependent oscillations in the optical activity of chiral molecules: the presence weak interactions would be revealed by oscillation of the optical activity around a non-zero value 🕮 M. Harris & Stodolsky, Phys. Lett. **78B**, 313 (1978)

- Look for violation of the selection rules in the time evolution of states of well-defined initial parity: 1) preparation of molecular states of well-defined parity; 2) free evolution of the isolated molecule with initial well-defined parity; 3) observation of the population states of the forbidden parity (created by the parity violating interactions) as a function of time 🕮 M. Quack, Chem. Phys. Lett. **132**, 147 (1986)

Constancy of constants

- Dirac's big-numbers hypothesis 🕮 P.A.M. Dirac, Nature **139**, 323 (1937)

  $G \sim t^{-1}$

- Generalized Kaluza-Klein models, String theories 🕮 J.-P. Uzan, Rev. Mod. Phys. **75**, 403 (2003)

$$R \sim l_P = \sqrt{\frac{\hbar G}{c^3}} \approx 1.62 \cdot 10^{-35}\ \mathrm{m} \qquad \dot{R} \neq 0 \Rightarrow$$

real changes in values of α, β,... take place

- Inflation Model 🕮 S.G. Karshenboim, Can. J. Phys. **83**, 767 (2005) 🕮 G. Börner, The Early Universe (Springer-Verlag, 1993)

expansion of the Universe → **cooling** → **phase transition** → **change in the electron charge/mass**

...the Universe is still expanding and cooling...

$$\alpha = \frac{e^2}{4\pi\varepsilon_0\hbar c}$$ **defines the QED scale**

$$\beta = \frac{m_p}{m_e}$$ **characterizes the strength of strong interaction in terms of the electro-weak**

Constraints on the fractional temporal variation of α (β) can be inferred from precise frequency comparisons of transitions with different sensitivities to α (β) 🕮 S.N. Lea, Rep. Prog. Phys. **70**, 1473 (2007)

Identifying the *Ingredients*: Outline

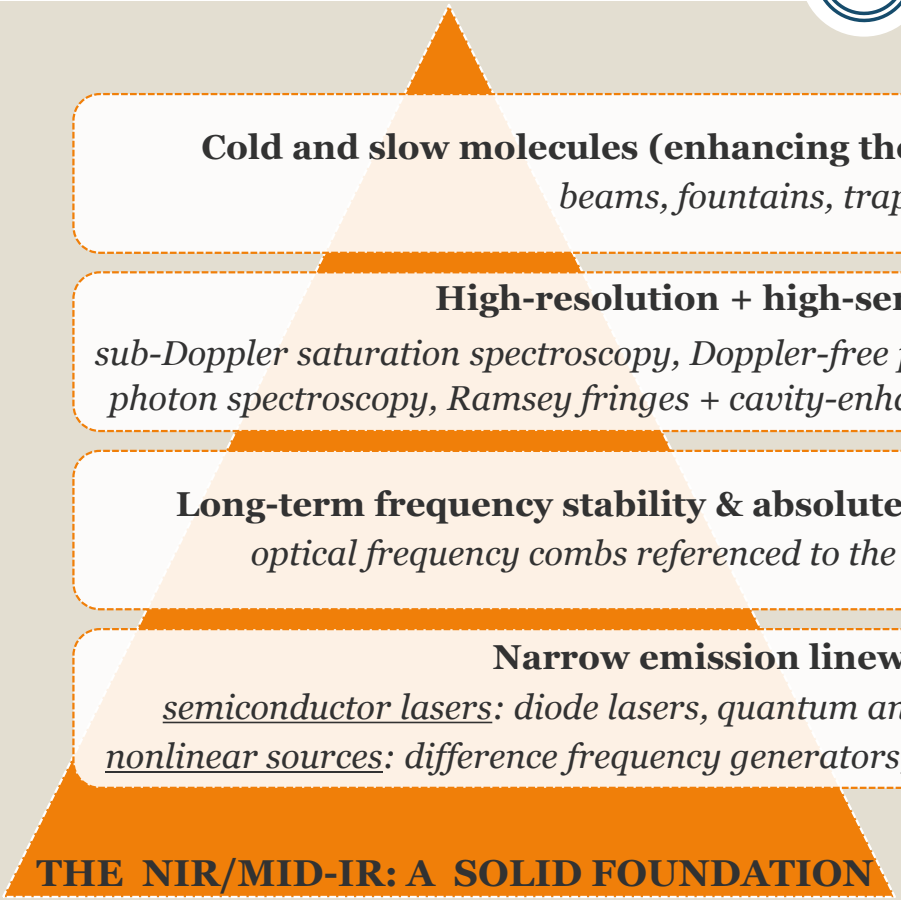

Improved samples

Interrogation techniques

Radiation Sources

- Strong vibrational transitions (up to 10^{-18} cm/molec) with reduced natural linewidths (down to a few Hz) + valuable laser sources and detectors

📖 P. Maddaloni et al., Laser-based measurements for time and frequency domain applications, Taylor&Francis (2013)

Cw Laser Sources and Optical Frequency Combs

LINKING ULTRA-NARROW-LINEWIDTH NIR/MIR PROBE LASER SOURCES TO THE CESIUM PRIMARY STANDARD

Direct semiconductor lasers

Conventional diode lasers:
… → 2.9 micron

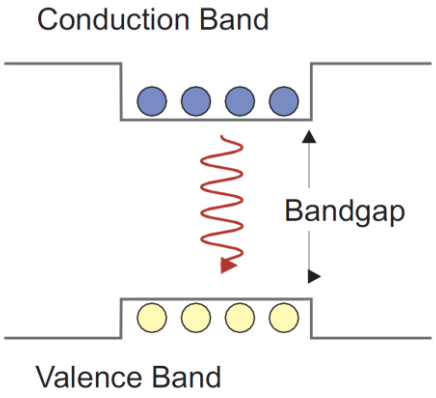

Quantum cascade lasers:
4 micron → …

J. Faist et al., Science **264**, 553 (1994)
R.F. Curl et al., Chem. Phys. Lett. 487, 1 (2010)

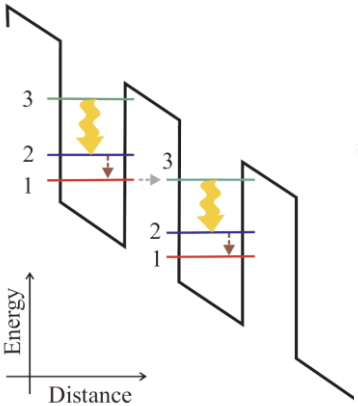

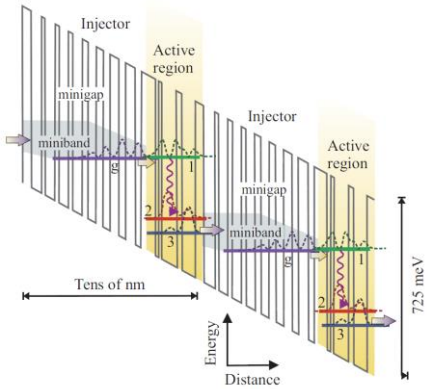

QCLs are unipolar devices, as they use only one type of charge carriers (electrons) which allow light emission by means of quantum jumps between conduction-band sublevels artificially created by structuring the active region in a series of quantum wells

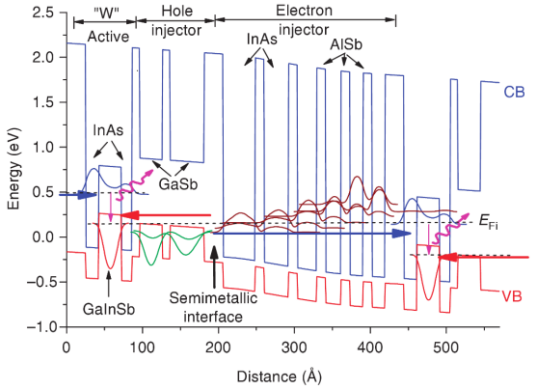

Interband cascade lasers
3 micron → 4 micron

ICLs also employ the concept of band-structure engineering to reuse injected electrons for emitting multiple photons, but photons are generated by interband rather than intersubband transitions

I. Vurgaftman et al., Nature Communications 2:585 (2011)

- ✓ Compactness, TE cooled
- ✓ Custom wavelength
- ✓ High power output (tens to hundreds of mW)
- ✓ Single mode emission (free-running linewidth of a few MHz)

Nonlinear laser sources

Difference frequency generator

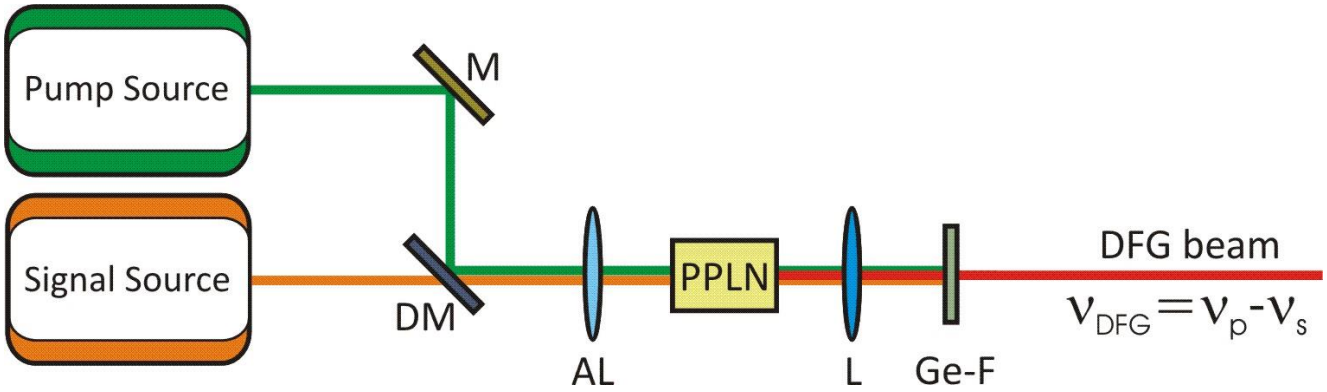

- ✓ Wide tunability
- ✓ Narrow linewidth (basically determined by that of the pumping sources)
- ✓ Relatively high power (< 10 mW)

Optical parametric oscillator

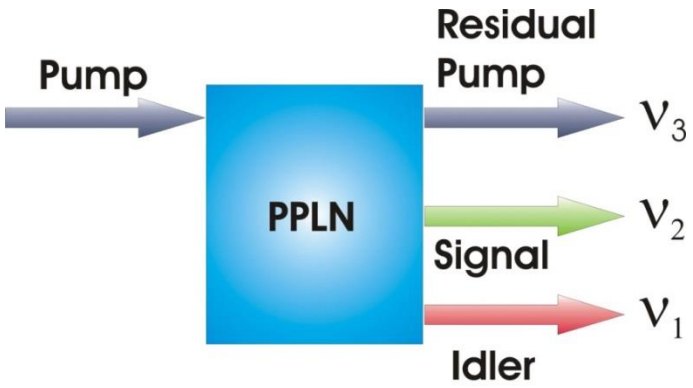

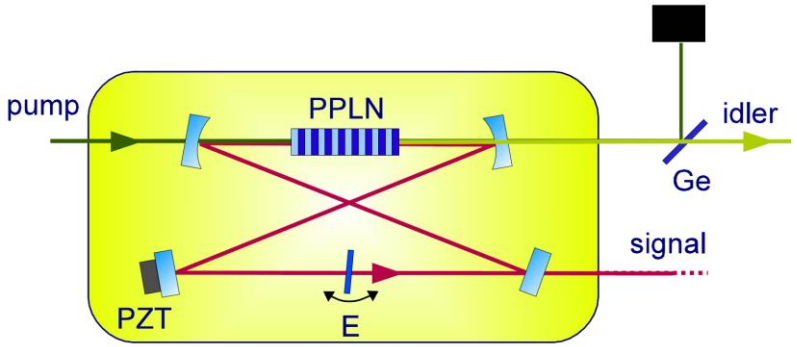

Much higher power, but cavity is needed to obtain frequency-stable and single-mode behaviour

📖 P. Maddaloni et al., Appl. Phys. Lett. **94**, 121105 (2009)

📖 I. Ricciardi et al., Mol. Phys. **110**, 2103 (2012)

Optical frequency combs

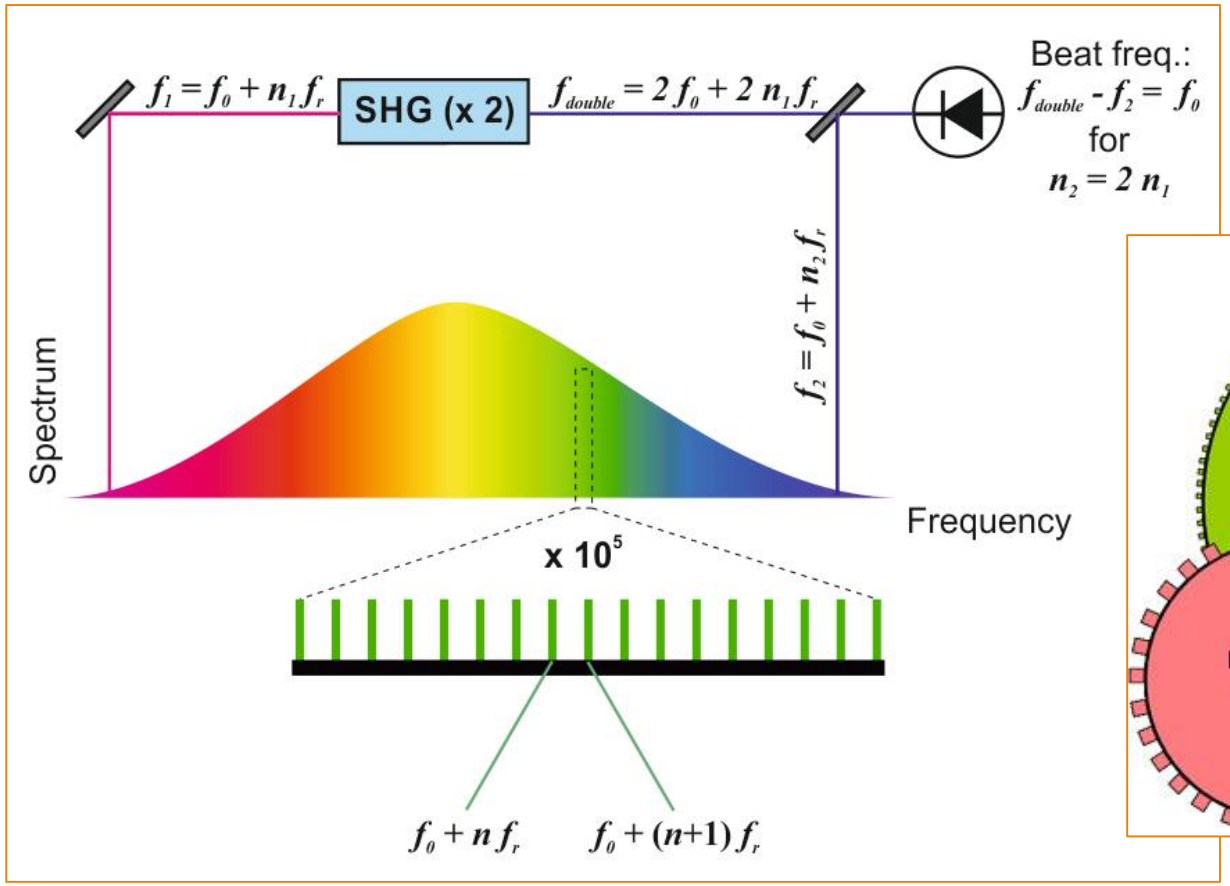

📖 D.J. Jones et al., Science **288**, 635 (2000)

📖 T. Udem et al., Nature **416**, 233 (2002)

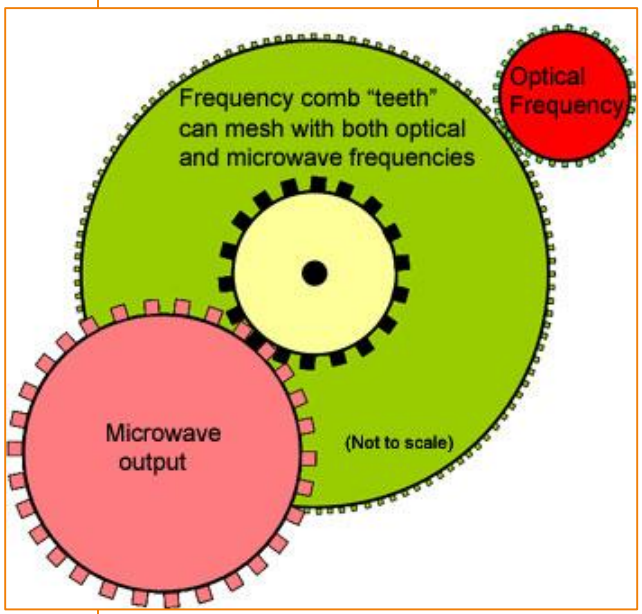

The second *is defined as the duration of 9,192,631,770 periods of the radiation corresponding to the transition between two hyperfine levels* $|F = 4, m_F = 0\rangle \leftrightarrow |F = 3, m_F = 0\rangle$ *in the ground state* $^2S_{1/2}$ *of the* ^{133}Cs *atom*

📖 P. Maddaloni et al., Meas. Sci. Technol. **20**, 052001 (2009)

📖 I. Ricciardi et al., Optics Express B **20**, 9178 (2012)

Comb-assisted laser spectroscopy

FC1500-250-WG Synthesizer
Er fiber oscillator
1050-2100 nm

FC8004 Synthesizer
Ti:Sa oscillator
500-1100 nm

Still limited to visible/near-infrared spectral region

(special sources and fibers required)

Extension to UV (MIR & FIR) ⇒

Frequency up (down) conversion based on nonlinear optical processes

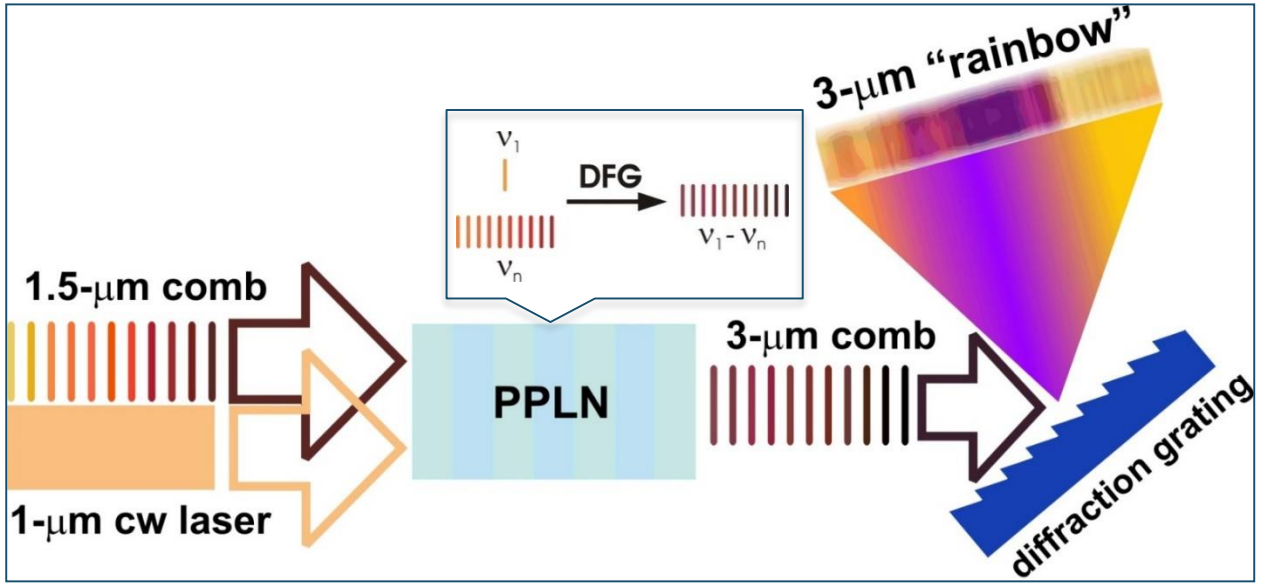

📖 P. Maddaloni et al., New Journal of Physics **8**, 262 (2006)

📖 P. Malara et al. Opt. Express **16**, 8056 (2008)

Direct comb referencing

$$f_{laser} = f_0 + n_{laser} f_r + f_{beat}$$

from RF counters (beat notes with a SNR>30 dB)

from wavemeter (accuracy better than $f_r/2$)

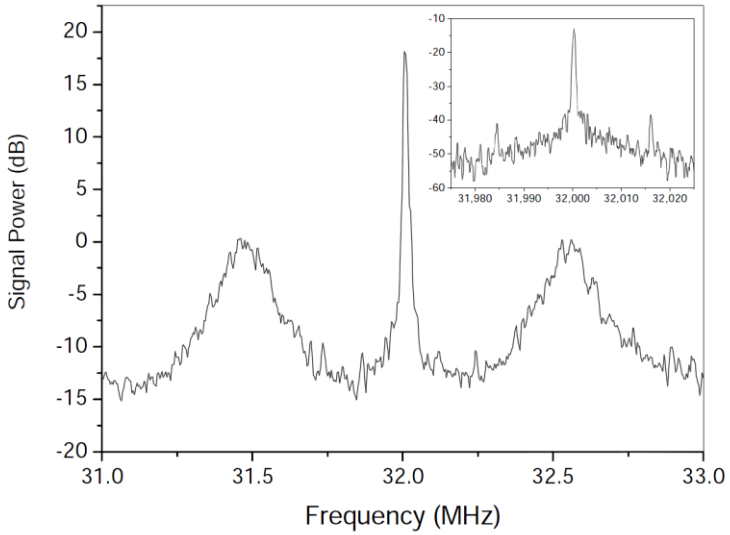

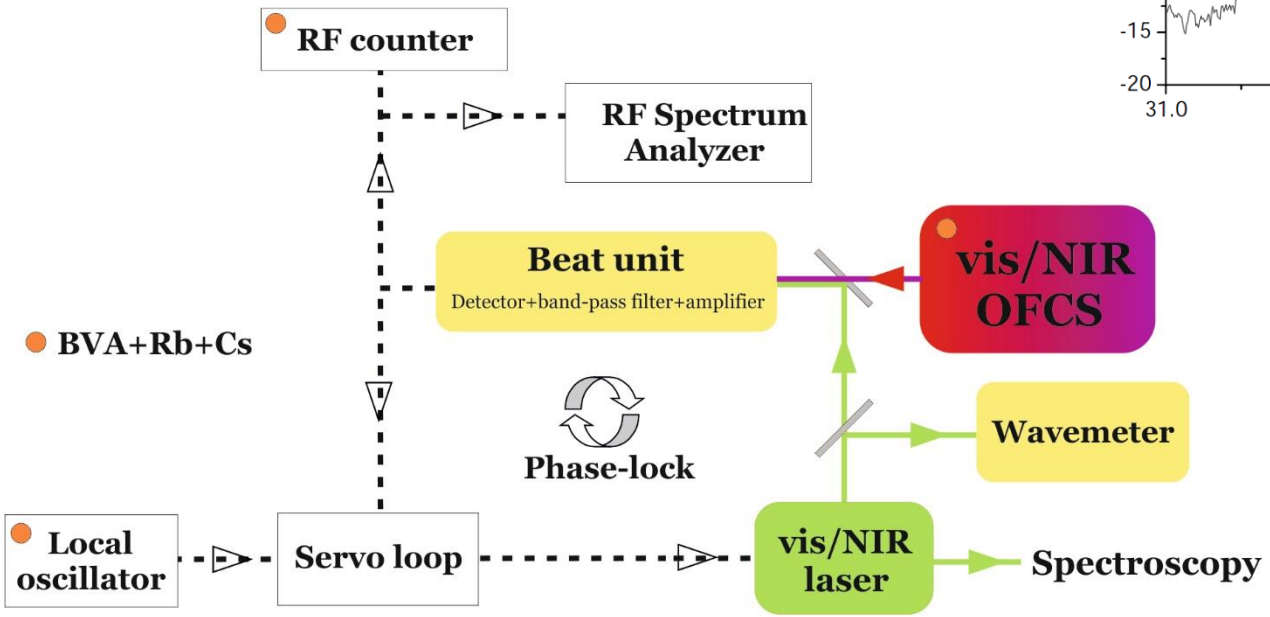

Phase-lock also narrows the laser linewidth down to that of the comb tooth

P. Cancio et al., Appl. Phys B **102**, 255 (2011)

Comb referencing of DFG/OPO sources

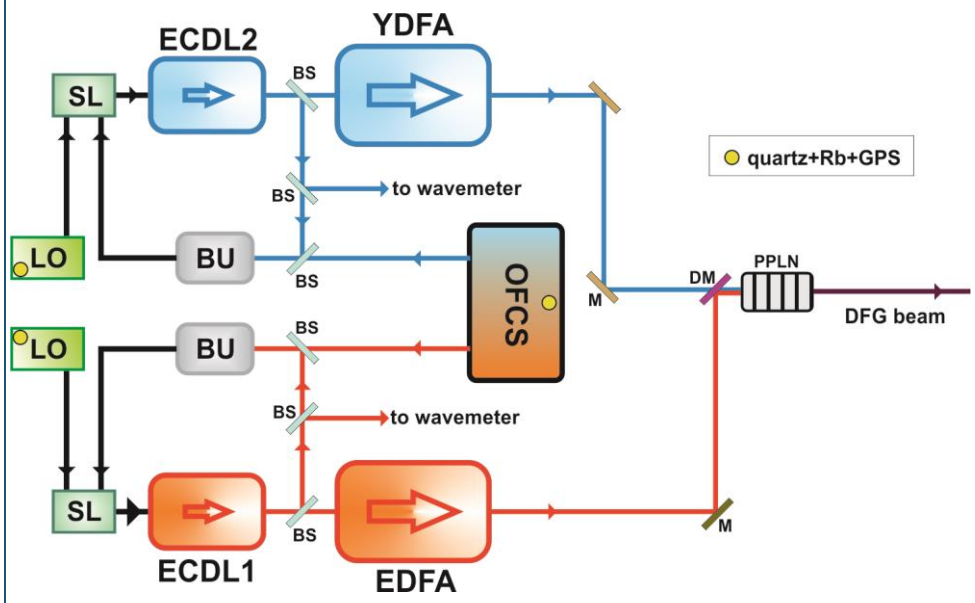

$$f_p = n_p f_r + f_0 + f^p_{beat}$$
$$f_s = n_s f_r + f_0 + f^s_{beat}$$

$$f_{DFG} \equiv f_p - f_s = (n_p - n_s) f_r + (f^p_{beat} - f^s_{beat})$$

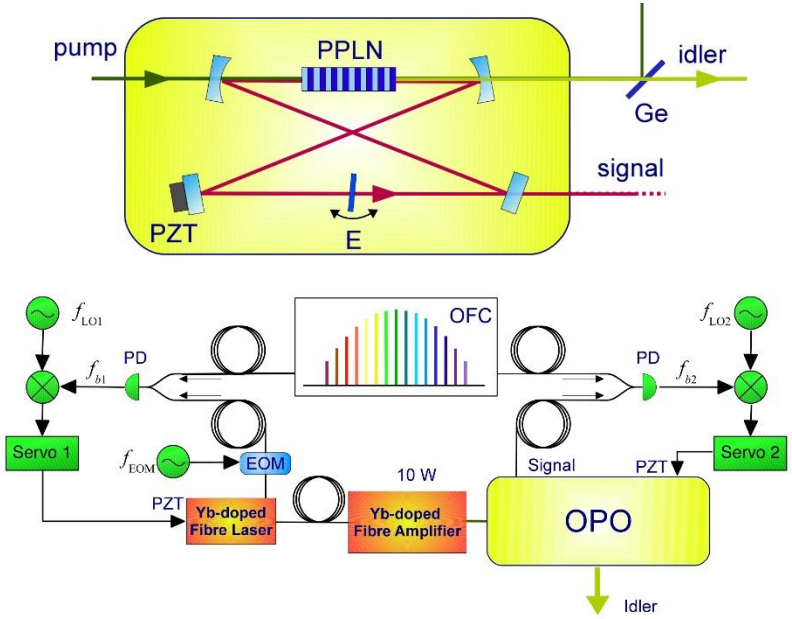

$$f_p - f_{EOM} = f_0 + n_p f_r + f^p_{beat}$$
$$f_s = f_0 + n_s f_r + f^s_{beat}$$

$$f_{OPO} = f_p - f_s = (n_p - n_s) f_r + (f^p_{beat} - f^s_{beat}) + f_{EOM}$$

📖 I. Ricciardi et al., Optics Express **21**, 14618 (2013)

P. Maddaloni et al., J. Chem. Phys. **133**, 154317 (2010)

Direct cooling of stable molecules

ACCESS TO HYDRIDES, NITRIDES, OXIDES, FLUORIDES,...

AS OPPOSED TO CREATION OF DIMERS VIA MAGNETO (PHOTO)-ASSOCIATION OF ULTRACOLD ALKALI ATOMS

Stark Deceleration

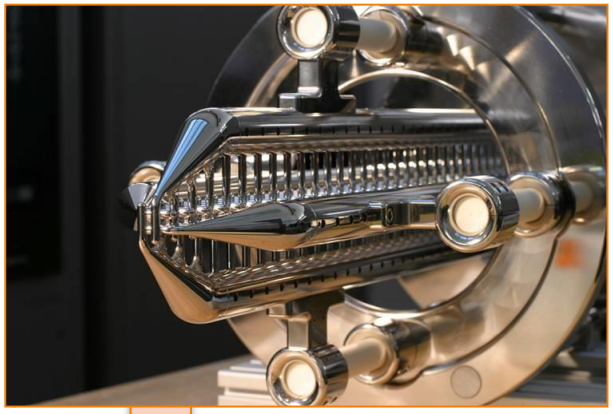

Stark effect

$$H = H_0 - \vec{\mu} \cdot \vec{\mathcal{E}}$$

H.L. Bethlem et al., Phys. Rev. Lett. **83**, 1558 (1999)

Hexapole lens

In linear regime, the hexapole provides a radial (velocity) confinement due to a quadratic potential

$$F_r = -k_{el} r$$

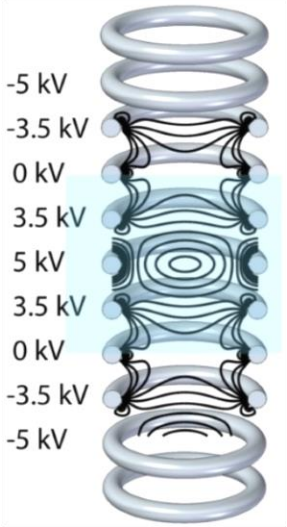

Hundreds of ring-shaped tantalum electrodes are connected in sets of 8. Oscillating high voltages are applied to these sets with a phase difference of 2π/8, thereby creating a series of electric field minima, which are true 3D traps for molecules in a low field seeking state.

$$V_n(t) = V_0 \sin\left[-\phi(t) + \frac{2\pi n}{8}\right]$$

$$v_z(t) = f(t)L = \frac{1}{2\pi}\frac{d\phi}{dt}L$$

The frequency of the voltages determines the velocity of the moving traps. Initially, as the molecules enter the decelerator, the traps are set to move at the same speed as the molecules. Then, gradually, the oscillation frequency of the voltages is swept down resulting in the deceleration and ultimately stopping of the traps, with the molecules remaining in the traps.

A. Osterwalder et al., Phys. Rev. A **81**, 051401(R) (2010)

Technologies borrowed from atoms

Magneto-optical trapping

📖 J.F. Barry et al., Nature **512**, 286 (2014)

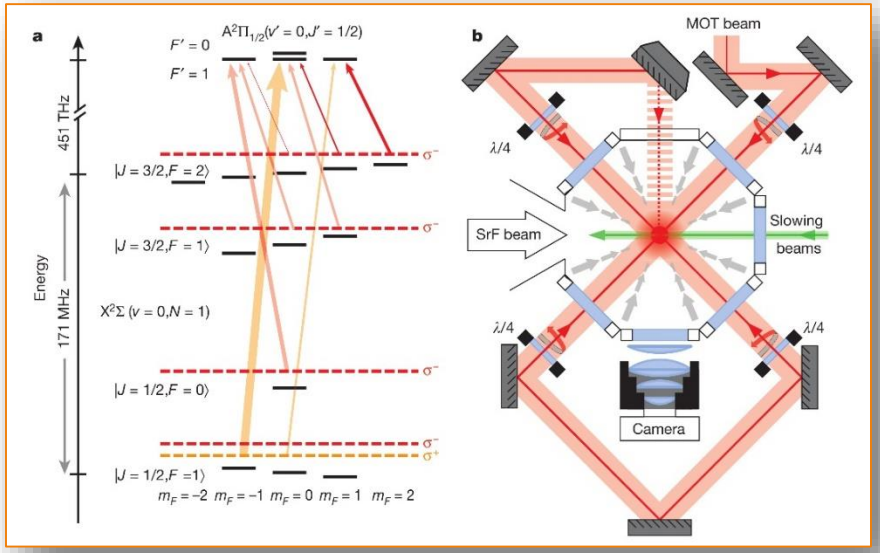

3D MOT of strontium monofluoride at a temperature of approximately 2.5 mK, loaded with pulses of SrF from a cryogenic buffer gas beam source that have been slowed using radiation pressure

Sysiphus cooling

📖 M. Zeppenfeld et al., Nature **491**, 570 (2012)

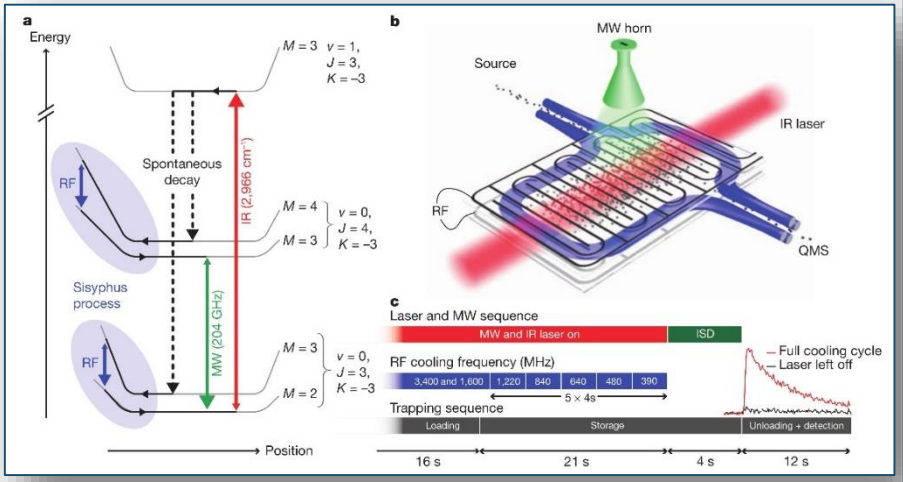

Radiation couples molecular states which experience a position-dependent potential energy in an mictrostructured electric trap. Molecules following the emphasized route lose more kinetic energy when entering the strong-field edge region of the trap than they regain when returning to the trap centre in a more weakly trapped state. Combined with the unidirectionality of the optical pumping back to the strongly trapped states, this cools about one million of CH_3F molecules by a factor of 13.5, with the phase space density increased by a factor of 29.

Evaporative cooling

📖 B.K. Stuhl et al., Nature **492**, 396 (2012)

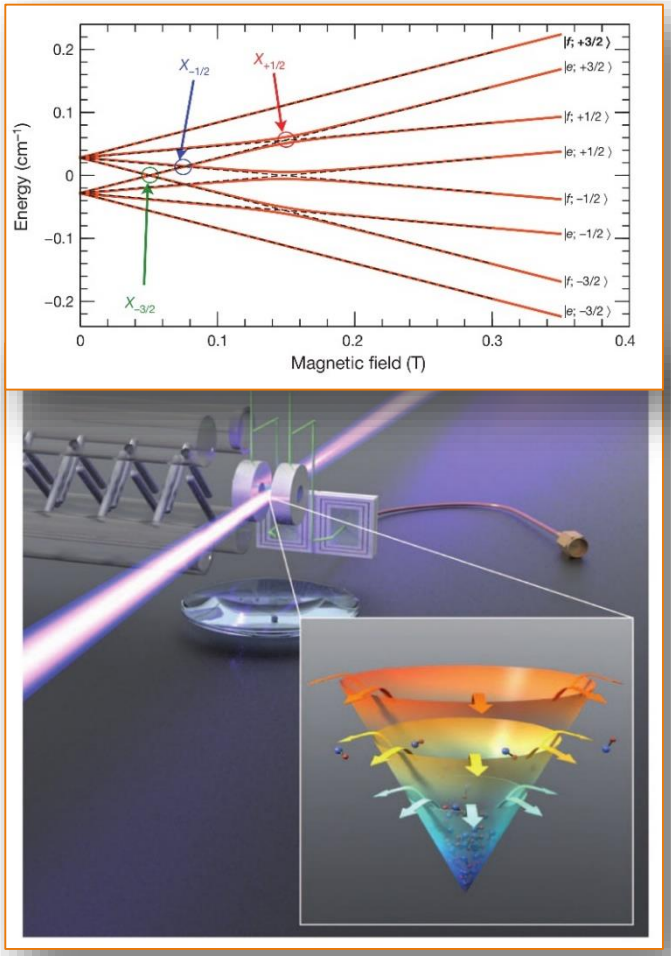

Microwave-forced evaporative cooling of neutral hydroxyl molecules loaded from a Stark-decelerated beam into a high-gradient magnetic quadrupole trap → cooling by one order of magnitude in temperature (correspondingly phase-space density increases by 3 orders of magnitude)

Symphatetic cooling

📖 W.G. Rellergert et al., Nature **495**, 490 (2013)

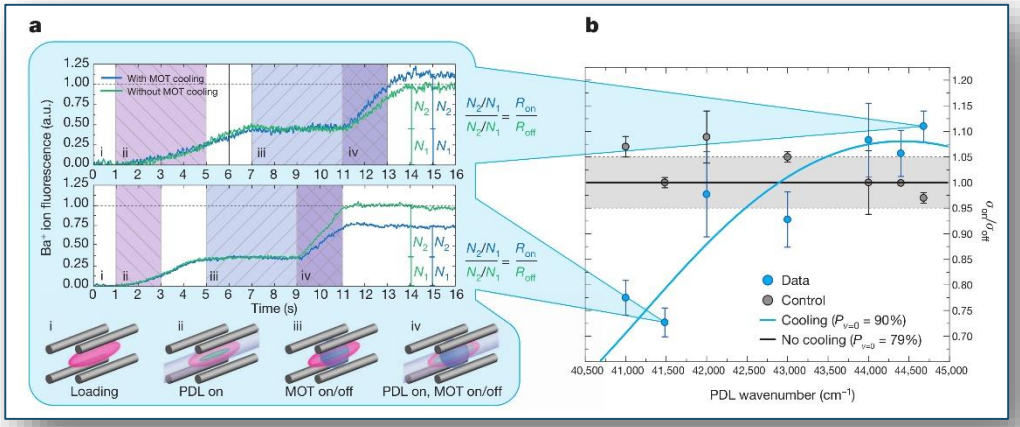

The vibrational motion of trapped $BaCl^+$ molecules is quenched by collisions with ultracold calcium atoms at a rate that is over four orders of magnitude more efficient than traditional sympathetic cooling schemes. The high cooling rate, a consequence of a strong interaction potential (due to the high polarizability of calcium), along with the low collision energies involved, leads to molecular samples with a vibrational ground-state occupancy of at least 90%. Because sympathetic cooling of molecular rotational motion is much more efficient than vibrational cooling in traditional systems, the method should also allow efficient cooling of the rotational motion of the molecules

Sounding the time **U**nwinding of the **PR**oton-to-**E**lectron **M**ass rati**O** - **SUPREMO**

INFN EXPERIMENT - CSN II

https://web.infn.it/supremo

Main goal

Constrain over a-few-year timescale the fractional temporal variation of the proton-to-electron mass ratio at a level of 10^{-15}/yr by means of a spectroscopic frequency measurement on a beam of cold and slow molecules

$$\beta = \frac{m_p}{m_e} \quad \Rightarrow \quad \frac{1}{\beta}\frac{d\beta}{dt} < 10^{-15}\ \mathrm{yr}^{-1}$$

- Possible validation of multidimensional theories seeking to unify the three distinct gauges of the Standard Model towards a GUT (Lie groups,…)

  📖 H. Fritzsch, Lect. Notes Phys. **648**, 107 (2004)

- Testing TOE-aspirant theoretical frameworks (String/M-theories, Loop quantum gravity,…) attempting to reconcile Standard Model and General Relativity

  📖 C. Kiefer, Lect. Notes Phys. **648**, 115 (2004)

State of the art

Hybrid Cosmological Approach

👍 **look-back time of several Gyr**

👎 **poor control on data**

	Transition	Energy scaling
Atomic	Gross structure	Ry
	Fine structure	$\alpha^2 Ry$
	Hyperfine structure	$\alpha^2(\mu/\mu_B)Ry$
Molecular	Electronic structure	Ry
	Vibrational structure	$\beta^{-1/2}Ry$
	Rotational structure	$\beta^{-1}Ry$
	Relativistic corrections	Function of α

All-Lab Approach

👎 **reduced look-back time**

👍 **accuracy, and reproducibility**

Compare wavelengths of atomic/molecular lines on Earth (at present epoch) and from astronomical objects at high redshifts (up to z≈3)

📖 P. Molaro, Highlights of Astronomy **15**, 326 (2010)

High-precision comparisons between transitions with different sensitivities to β

📖 S.N. Lea, Rep. Prog. Phys. **70**, 1473 (2007)

$\Delta\beta/\beta=(0.0\pm1.0)\cdot10^{-7}$ z=0.89 (7 Gyr)

📖 J. Bagdonaite et al., Science **339**, 46 (2013)

$\dot{\beta}/\beta=(-3.8\pm5.6)\cdot10^{-14}$ yr^{-1}

📖 A. Shelkovnikov et al., Phys. Rev. Lett. **100**, 150801 (2008)

The proposal

Measure the frequency of a molecular ro-vibrational transition relative to the Cs clock hyperfine transition

$$\frac{1}{\frac{\nu(M)}{\nu(Cs)}}\frac{\partial\left[\frac{\nu(M)}{\nu(Cs)}\right]}{\partial t} = -\frac{1}{2\beta}\frac{\partial\beta}{\partial t} - 2.83\frac{1}{\alpha}\frac{\partial\alpha}{\partial t} - \frac{1}{\frac{\mu_{Cs}}{\mu_B}}\frac{\partial\left(\frac{\mu_{Cs}}{\mu_B}\right)}{\partial t}$$

$$\frac{\dot{\alpha}}{\alpha} = (-1.6 \pm 2.3)\cdot 10^{-17}\ \text{yr}^{-1}$$

$$\frac{d}{dt}\ln\frac{\mu_{Cs}}{\mu_B} = (-1.9 \pm 4.0)\cdot 10^{-16}\ \text{yr}^{-1}$$

A. Shelkovnikov et al., Phys. Rev. Lett. **100**, 150801 (2008)

L. Lorini et al., Eur. Phys. J. Special Topics **163**, 19 (2008)

Increase the spectroscopic interrogation time by exciting 2-photon Ramsey fringes

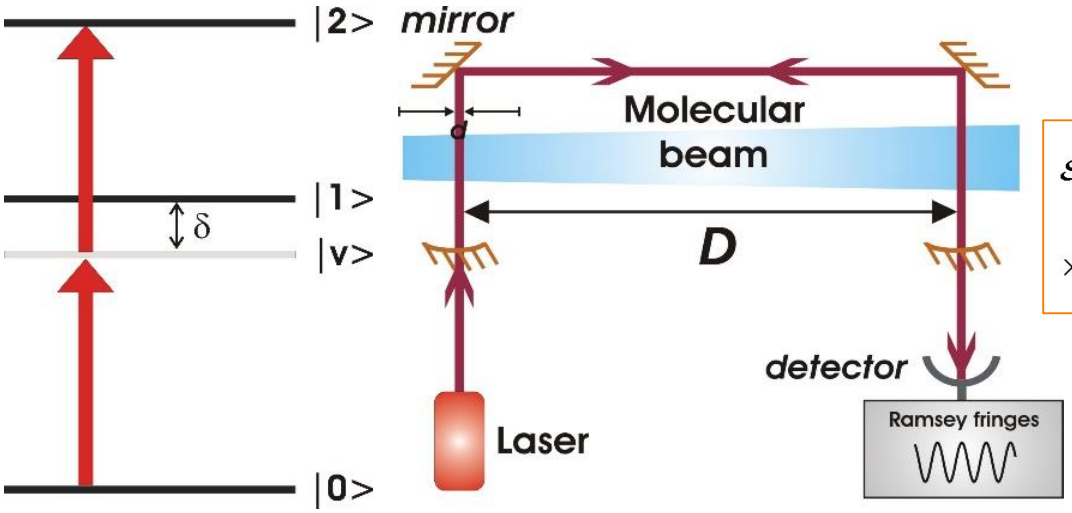

Decrease fringe periodicity & increase fringe contrast

$$\mathcal{S}(\omega,T) \sim p_0(T)\left[\frac{\mu_{21}\mu_{10}I_L}{\delta}\frac{d}{u}\right]^2 \times \int_0^\infty \left[1 + e^{-2\gamma\frac{D}{u}} + 2e^{-\gamma\frac{D}{u}}\cos\frac{(2\omega-\omega_{20})D}{u}\right]\mathcal{F}(\Delta u)\,du$$

Use a beam of slow, translationally and rotationally cold molecules

L. Santamaria et al., J. Mol. Spectrosc. **300**, 116 (2014)

Molecular candidates: CF_3H, H_2CO

Fluoroform

Symmetric top (C_{3v})

Perm. EDM=1.65 Debye

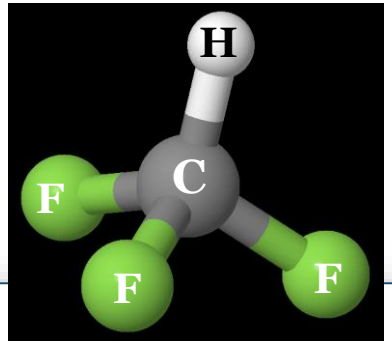

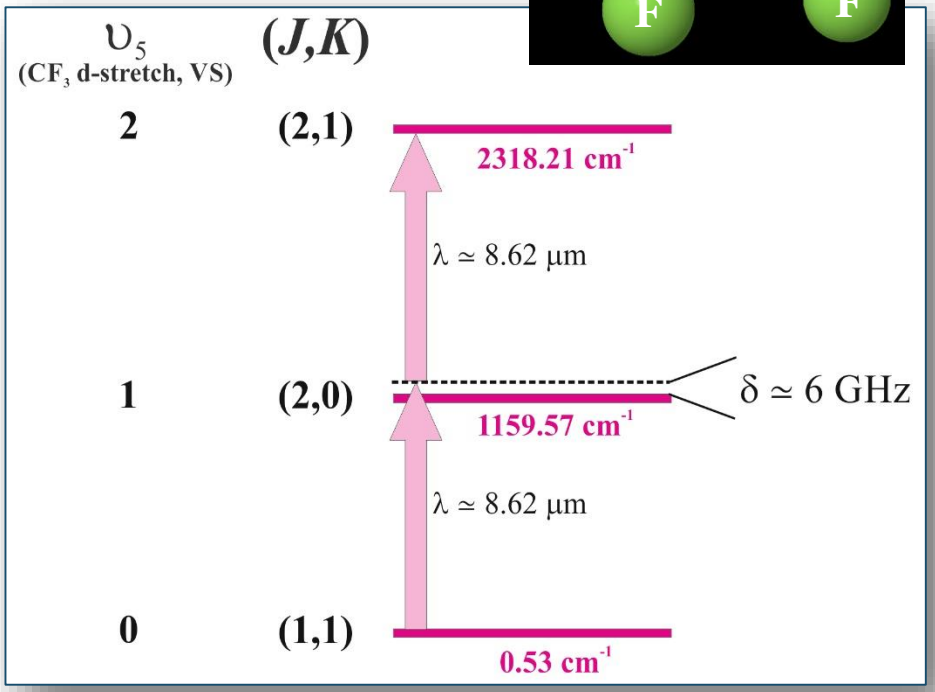

Formaldehyde

Plane symm. Y form (C_{2v})

Perm. EDM=2.34 Debye

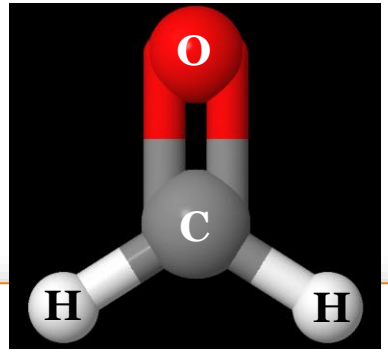

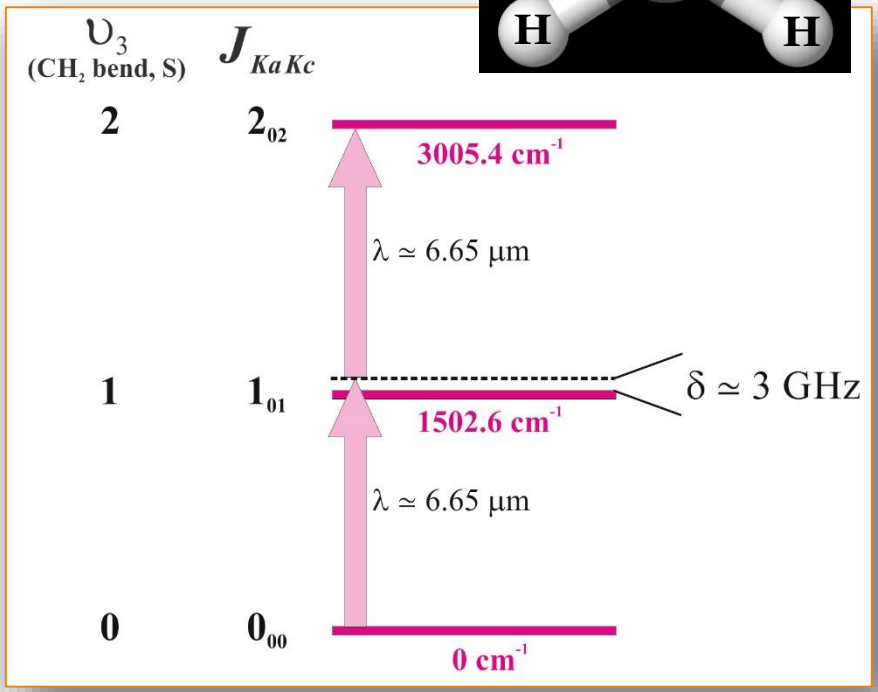

Buffer Gas Cooling

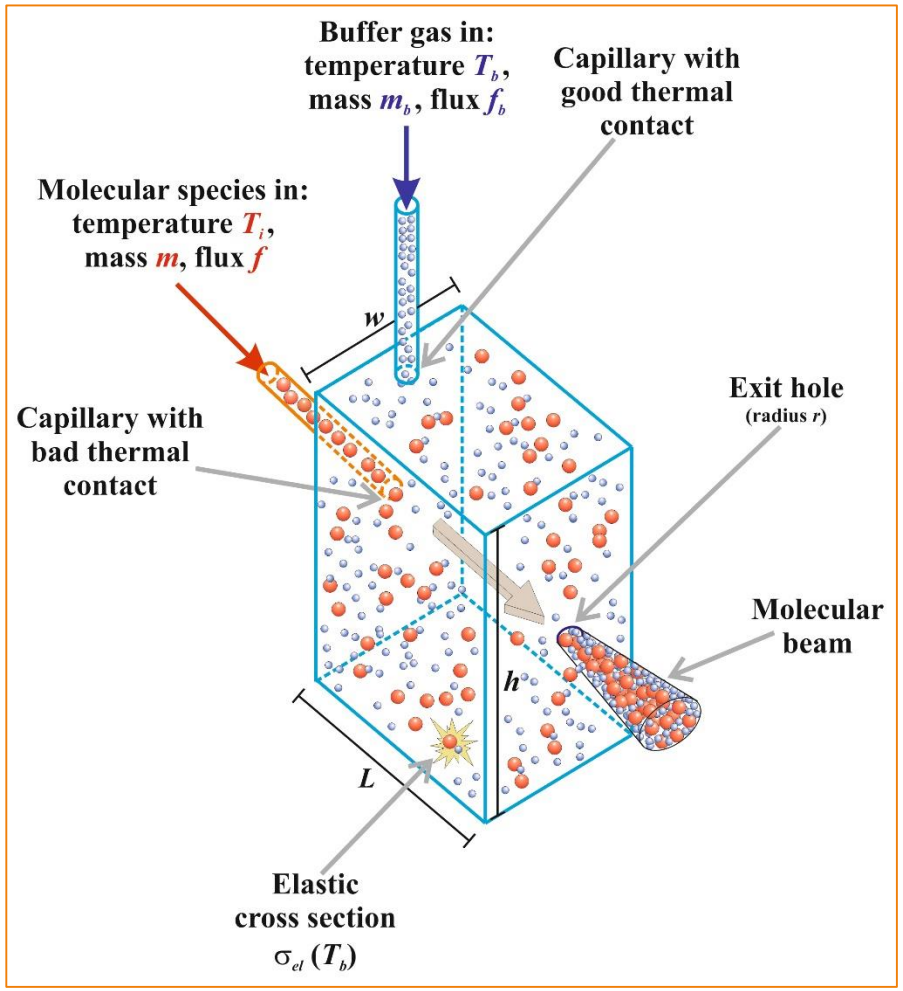

Both translational and rotational (internal) degrees of freedom of the desired molecular species are cooled via collisions with a thermal bath of helium in a cryogenic cell

📖 S.E. Maxwell et al., Phys. Rev. Lett. **95**, 173201 (2005)

📖 N.R. Hutzler et al., Chem. Rev. **112**, 4803 (2012)

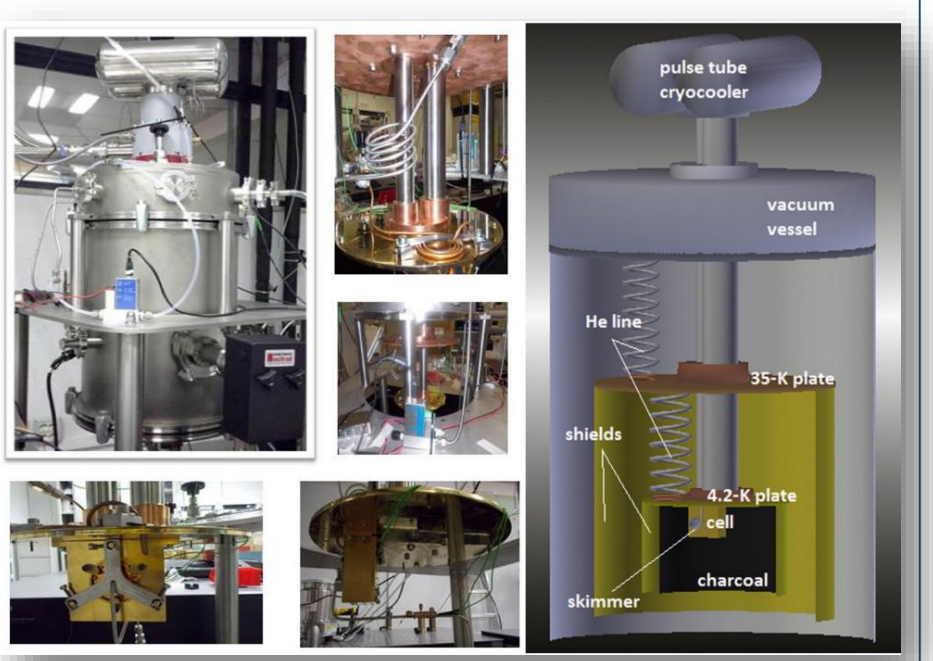

Molecular Beam Parameters

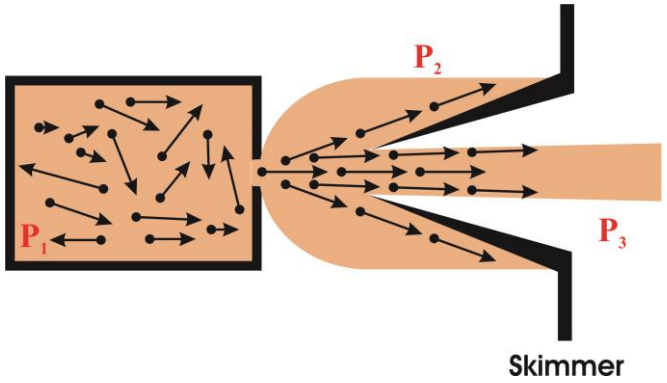

Effusive beam	$Re < 1$	$\Delta\theta \approx 120°$
Partially hydrodynamic	$1 < Re < 100$	lower divergence
Supersonic beam	$Re > 100$	$\Delta\theta \approx 78°$

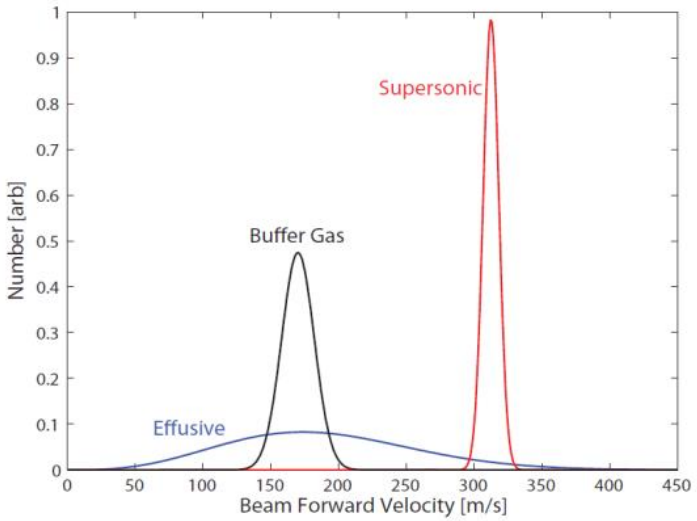

Reduced mean forward velocity (u) and temperature (i.e. spread around u, Δu)

$$Re \equiv \frac{F_{inert}}{F_{viscous}} \simeq \frac{8\sqrt{2}\, f_b\, \sigma_{b-b}}{\sqrt{\frac{8k_BT_b}{\pi m_b}}\, r} \qquad \sigma_{b-b} \simeq 3 \cdot 10^{-19}\ \mathrm{m}^2$$

$$1 \leq Re \leq 10$$

$$u \simeq \sqrt{\frac{8k_BT_b}{\pi m}} \left(1.2 + 0.6\, Re \sqrt{\frac{m_b}{m}}\right)$$

$$\Delta u \simeq \Delta v_\perp \simeq 1.5 \sqrt{\frac{8k_BT_b}{\pi m}}$$

$$\Delta\theta = 2 \arctan\left(\frac{\Delta v_\perp}{u}\right) \simeq 2 \arctan\left(\frac{1.5}{1.2 + 0.6\, Re \sqrt{\frac{m_b}{m}}}\right)$$

Characterizing the collisional cooling process

Laser-absorption ro-vibrational spectroscopy of the $^{12}C_2H_2$ ($\upsilon_1 + \upsilon_3$) band is performed

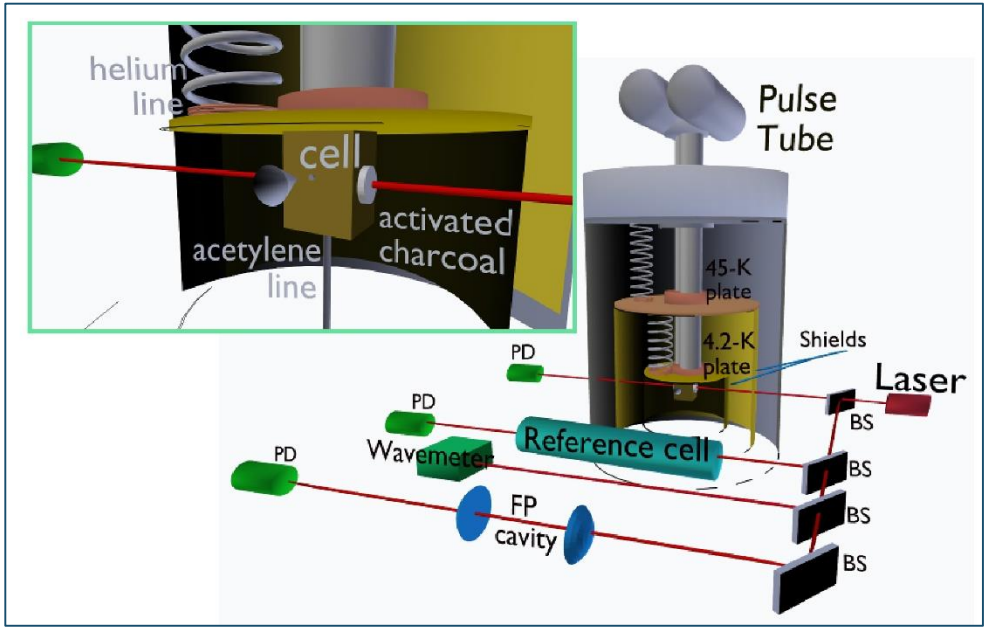

Due to a non perfect thermal exchange between the copper pipe and the two PT plates, a temperature of about 15 K is measured on the He line just before the entrance into the BGC cell (at 4.2 K); to bridge this gap, an improved setup for better cooling of the He line is under construction

Translational temperatures are extracted by Doppler thermometry

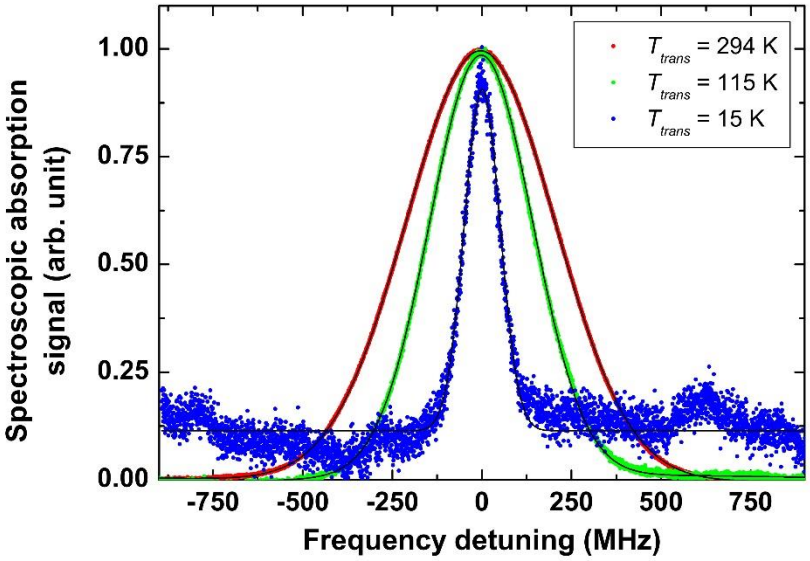

$$G(\nu) = G_0 \exp\left[-\frac{4\ln 2\,(\nu-\nu_0)^2}{\sigma_D^2}\right]$$

$$\sigma_D = \frac{\nu_0}{c}\sqrt{\frac{8\ln 2\,k_B\,T_{trans}}{m}}$$

L. Santamaria et al., The Astrophysical Journal **801**, 50 (2015)

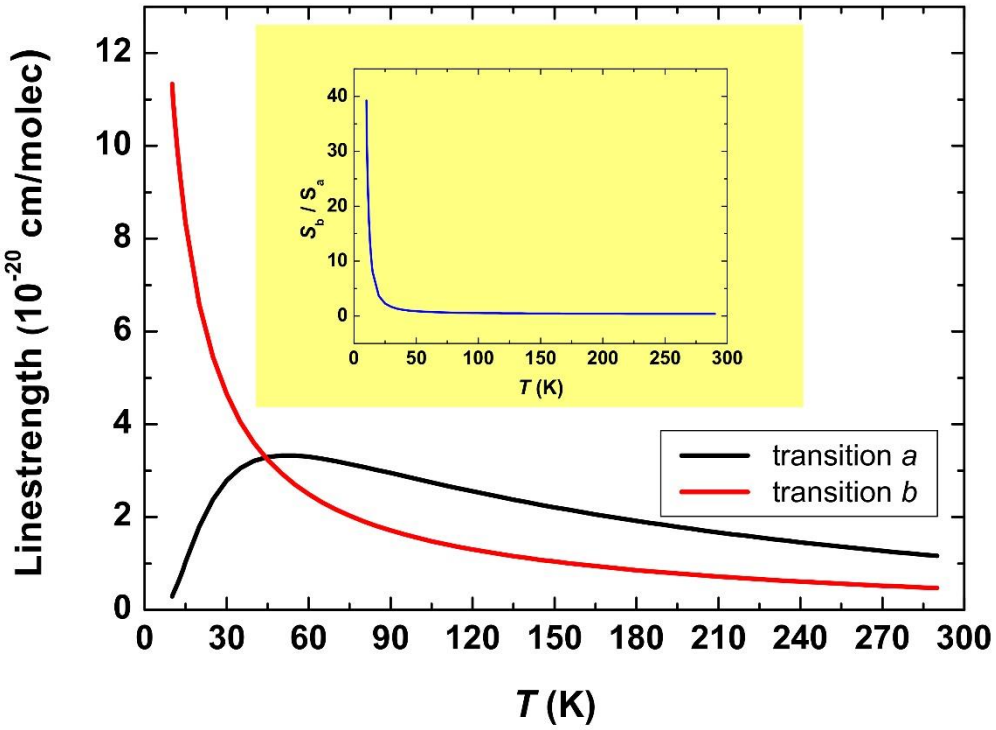

Rotational temperatures are retrieved by fitting the Boltzmann distribution to the relative intensities of several rotational lines

$$R_{ba}(T) \equiv \frac{S_b(T)}{S_a(T)} = \frac{\frac{\exp\left(\frac{-c_2 E_{fb}}{T}\right)}{\exp\left(\frac{-c_2 E_{fb}}{T_{ref}}\right)} \frac{1-\exp\left(\frac{-c_2 \nu_{0b}}{T}\right)}{1-\exp\left(\frac{-c_2 \nu_{0b}}{T_{ref}}\right)}}{\frac{\exp\left(\frac{-c_2 E_{fa}}{T}\right)}{\exp\left(\frac{-c_2 E_{fa}}{T_{ref}}\right)} \frac{1-\exp\left(\frac{-c_2 \nu_{0a}}{T}\right)}{1-\exp\left(\frac{-c_2 \nu_{0a}}{T_{ref}}\right)}}$$

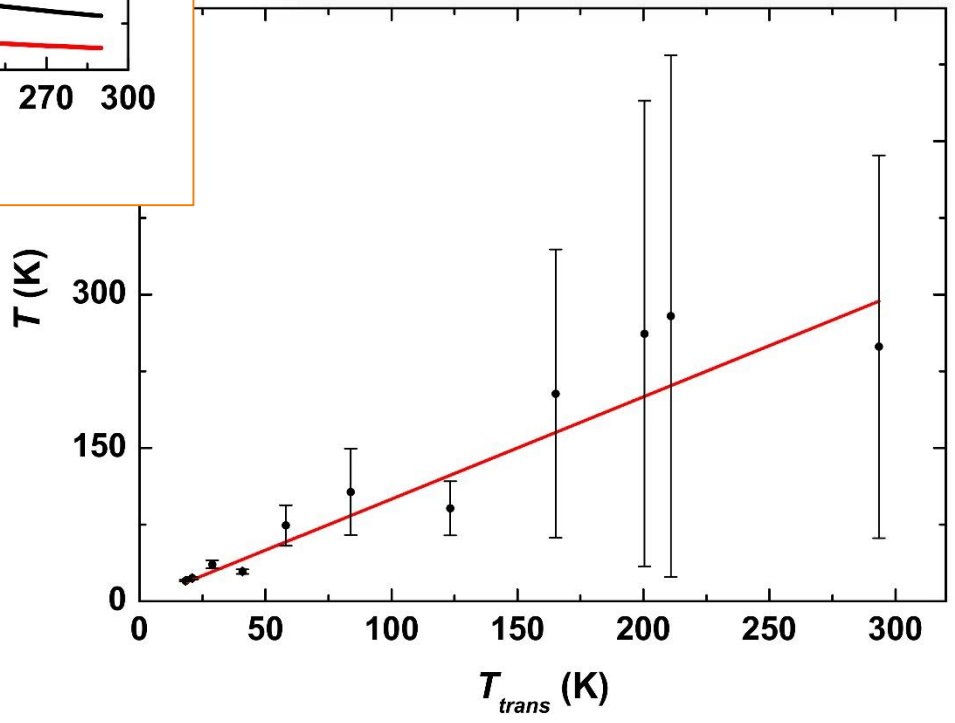

The minimum observed rotational temperature is T = (20±1) K for a measured translational temperature of T_{trans} = (15±3) K; such a difference is compatible with the fact that cooling is more efficient for the translational degrees of freedom than for rotational ones, albeit the two measured temperature values are consistent within 2 standard deviations.

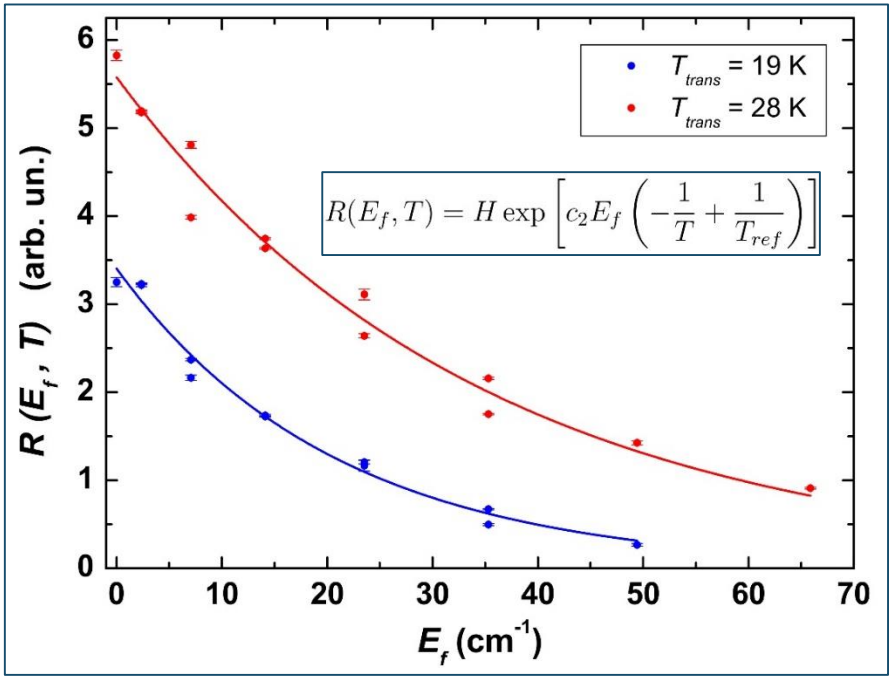

In general, unlike what happens to translational states, even if the initial distribution over the rotational states is Boltzmannian, it will relax without preserving the canonical invariance, and it will not be possible to define a rotational temperature. To address this issue in our case, a normalized linestrength is measured for several ro-vibrational lines at a given translational temperature. The acquired behavior is then compared with the theoretical line dictated by the Boltzmann law. In both cases, the correlation coefficient is $\chi = 0.98$, consistent with the hypothesis of canonical invariance.

The diffusion time of $^{12}C_2H_2$ in the BGC cell is measured against the ^{4}He flux both at two separate translational temperatures: 100 and 25 K. The observed behavior is compared with that predicted by a Monte Carlo simulation to provide an estimate for the respective total elastic cross sections:

$$\sigma_{el} = (100\ \mathrm{K}) = (4 \pm 1) \cdot 10^{-20}\ \mathrm{m}^2$$

$$\sigma_{el} = (25\ \mathrm{K}) = (7 \pm 2) \cdot 10^{-20}\ \mathrm{m}^2$$

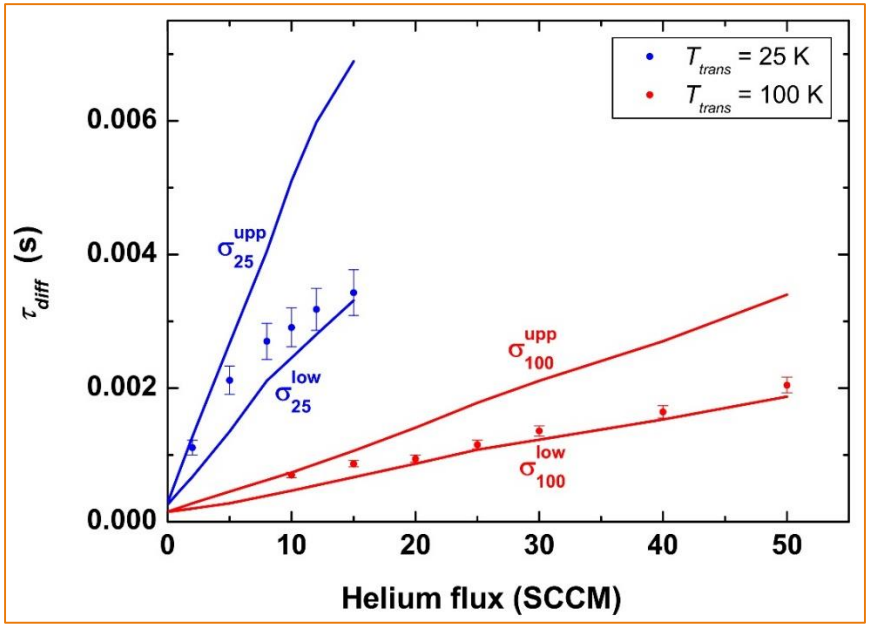

Characterization of the beam parameters (flux and velocities) by cavity ring-down spectroscopy

Schematic layout of the whole setup

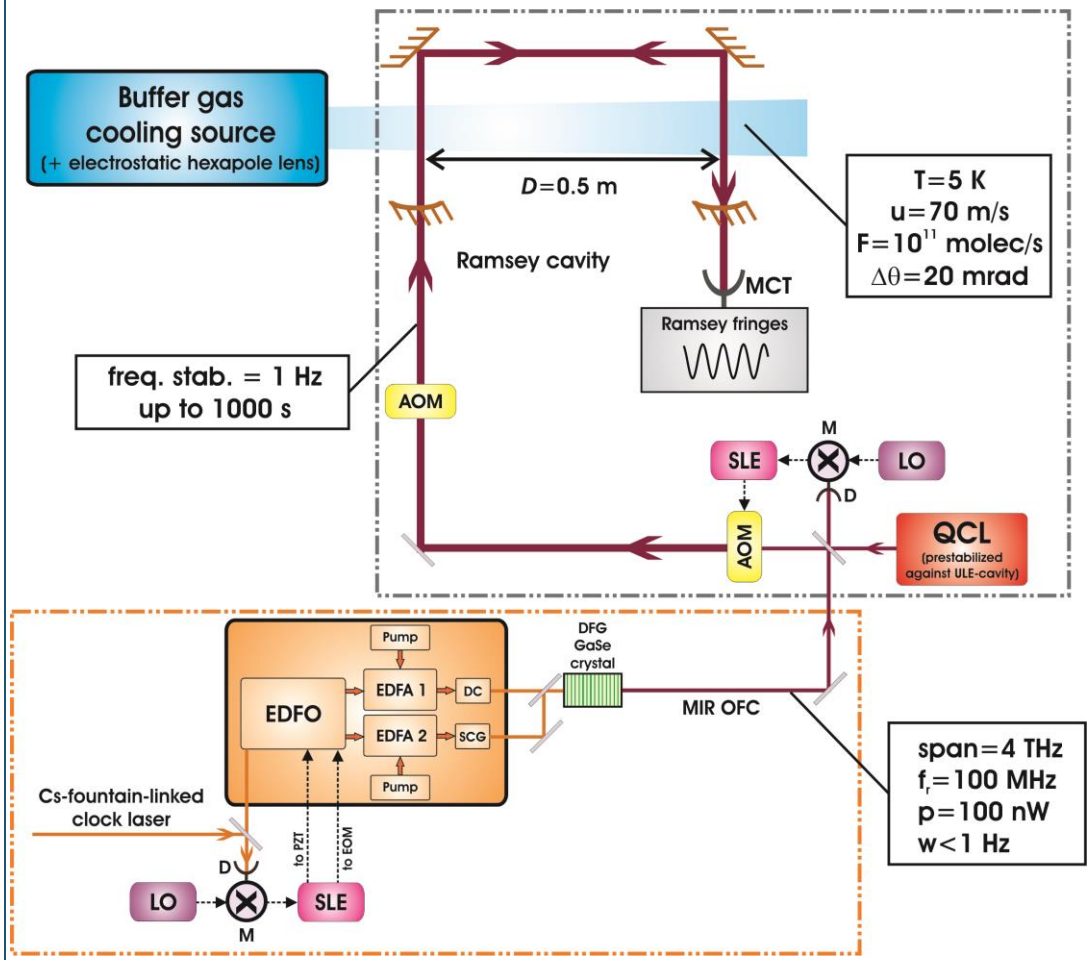

The cold fluoroform (CF_3H) beam is extracted from a buffer-gas-cooling source (and then collimated by means of an electrostatic hexapole lens). Employed in a 2-photon Ramsey-fringes interrogation, the probe source is a mid-infrared quantum cascade laser at 8.63 micron, phase-locked to a specially-developed optical frequency comb (OFC) that is ultimately referenced to the cesium primary standard via the National optical fiber link.

$$\mathcal{P} = \frac{u}{2D} = 35 \text{ Hz} \qquad SNR = 25,\ N_{\text{avg}} = 100$$

$$\mathcal{R} \sim \frac{\mathcal{P}}{SNR \cdot \sqrt{N_{\text{avg}}}} = 140 \text{ mHz}$$

$$4 \cdot 10^{-15}$$

National Optical Fiber Link

GPS limits the comb accuracy to $5 \cdot 10^{-12}$

→ improved primary standard

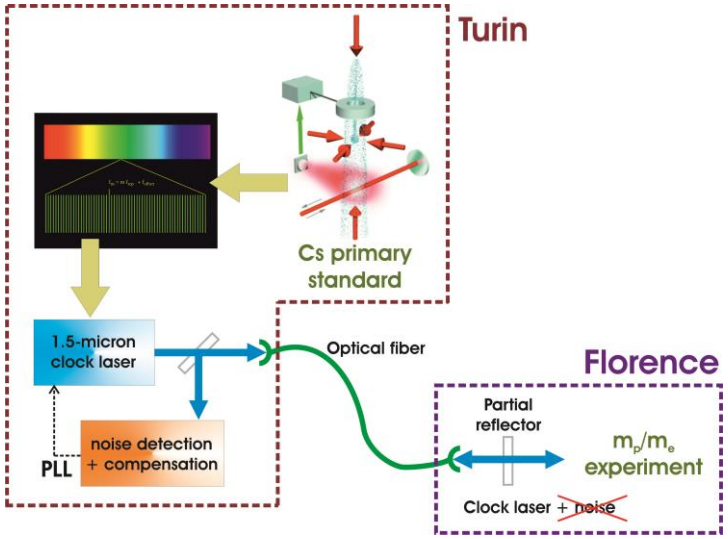

Istituto Nazionale di Ricerca Metrologica

A 1.5-micron laser, continuosly referenced to the primary Cs fountain via an OFC, is disseminated through a long optical fiber. Part of the laser radiation is reflected back and used to cancel the phase noise accumulated during the fiber propagation

Accuracy=$3 \cdot 10^{-16}$ **Stability=$3 \cdot 10^{-14} / \tau^{1/2}$**

📖 D. Calonico et al., Appl. Phys. B **117**, 979 (2014)

Pushing the ultimate resolution in the spectroscopic frequency measurement down to 10^{-18} by stabilizing the frequency comb, to which the probe laser is referenced, against an optical atomic standard

→ Yb lattice clock under construction at INRIM

$$\frac{1}{\frac{\nu_{vib}(M)}{\nu_{el}(Yb)}} \frac{\partial \left[\frac{\nu_{vib}(M)}{\nu_{el}(Yb)}\right]}{\partial t} = -0.5\frac{\dot{\beta}}{\beta} - N_{Yb}\frac{\dot{\alpha}}{\alpha}$$

Team and Collaborations

FIRENZE (INO & INFN)
Stark decelerated beam and REMPI spectroscopy

Giacomo Insero
Gabriele Santambrogio
Simone Borri
Paolo De Natale

NAPOLI (INO & INFN)
Precision spectroscopy and buffer gas cooling

Luigi Santamaria
Valentina Di Sarno
Gianpiero Mangano
Iolanda Ricciardi
Simona Mosca
Maria Parisi
Maurizio De Rosa

TORINO (INRIM)
National optical fiber link

Davide Calonico
Filippo Levi
Massimo Inguscio

BOLOGNA (UNIBO)
Molecular theory

Cristina Puzzarini

WASHINGTON, DC (NRL)
Interband cascade lasers

Jerry Meyer